Conformation of Native Antibody-Drug Conjugate Charge Variants Revealed by Microchip Capillary Electrophoresis Coupled with Trapped Ion Mobility

Eli J. Larson[1], Adi M. Kulkarni[2], Jake A. Melby[1], Matthew Fischer[1], Zhan Gao[1], Kevin M. Buck[1], Melissa R. Pergande[1], Yanlong Zhu[1], Guillaume Tremintin[3], Kate Yu[2], Ying Ge[1]

[1]University of Wisconsin-Madison, [2]908 Devices Inc., [3]Bruker Daltonics

WP 040

Overview

- **Rapid charge variant separation of mAbs and ADCs by microchip capillary electrophoresis coupled with trapped ion mobility mass spectromery.**
- **Conformational changes and alterations of average drug-to-antibody ratio were observed among charge variants along with changes in the collisional cross section between mAbs and ADCs.**

Introduction

Antibody-based therapeutics have become one of the largest drug classes recently, fueled by the therapeutic efficacy of monoclonal antibodies (mAbs) and antibody-drug conjugates (ADCs). However, mAb and ADC drug products are heterogeneous and susceptible to formation of charge variants that may increase the rate of proteolytic degradation, alter conformation and pharmacokinetics, or likelihood of aggregate formation[1]. For the first time, we present a native charge variant analysis by Microchip capillary electrophoresis (CE)[2] coupled with trapped ion mobility spectrometry[3] and mass spectrometry (CE-TIMS-MS) for four antibodies: NISTmAb, a native cysteine-linked ADC and its parent mAb, and lysine-linked ADC (Kadcyla). The developed method measures gas phase collisional cross section ($^{TIMS}CCS_{N2}$) for conformational state assessment of individual charge variants in only 10 minutes time. Our developed method enables rapid $^{TIMS}CCS_{N2}$ measurement for individual mAb and ADC charge variant species to assess potential conformation changes. This method revealed significant changes in charge variant $^{TIMS}CCS_{N2}$ between the unmodifed and deamidated model thereapeutic mAb peak, supporting previous spectroscopic investigations of the impact of mAb deamidation on conformation[4,5]. This method also partially separates DAR species of the lysine-linked ADC for MS analysis of the extremely complex drug products, a feat not possible by previously developed direct infusion TIMS-MS[3]. The native CE-TIMS-MS platform improves MS signal-to-noise relative to direct infusion, eliminates the need for sample clean up prior to injection, and uses <2 ng sample per analysis. This platform determines quality attributes such as intact mass, $^{TIMS}CCS_{N2}$, and average DAR for individual charge variant species in only 10 minutes.

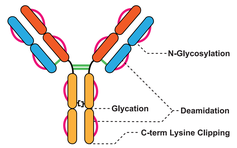

Scheme 1. Common causes of antibody charge variants.

Workflow

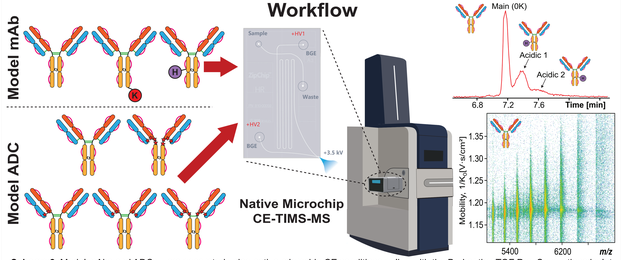

Scheme 2. Model mAbs and ADCs were separated using native microchip CE conditions online with the Bruker timsTOF Pro. Separations isolated charge variants for individual assesment of conformation by TIMS to enable charge variant specific $^{TIMS}CCS_{N2}$ information to be obtained.

Methods

Charge variants of a model cysteine-linked ADC, model lysine-linked ADC, and their respective parent mAbs were separated by a ZipChip Microchip CE Device (908 Devices) coupled with a Bruker timsTOF Pro for $^{TIMS}CCS_{N2}$ and intact mass measurement. Using a High Resolution Native chip and Charge Variant TOF background electrolyte, charge variants of the ADCs and parent mAbs were separated with a field strength of 500 V/cm and a 10-minute total runtime. 1 nL of sample was pressure injected, with ADCs at a concentration of 2 mg/mL and the mAbs at 1 mg/mL. The use of TIMS allowed calculation of $^{TIMS}CCS_{N2}$ for all mAbs and ADCs at the 26+ charge state using the Mason-Schamps equation (Equation 1)[6]. Where μ is the reduced mass of the ion, k_b is Boltzmann's constant, T is the drift region temperature, z is the ionic charge, e is the charge of an electron, N_0 the buffer gas density, and K_0 is the reduced mobility. Data analysis was performed using Compass DataAnalysis 5.3 and MASH Native v1.1. The average DAR for individual regions was determined by Maximum Entropy deconvolution with a resolution of 10,000 followed by Sum Peak peak picking to calculate the area under the curve for all observed DAR species (Equation 2). Where the area under the curve for all observed DAR species weighted by drug load is divided by the total unweighted area under the curve for all DAR species. For the model cysteine-linked ADC, odd numbered drug loading was not observed and the contribution of odd numbered DAR species was not included in the average DAR calculation.

Equation 1 $$^{TIMS}CCS_{N2} = \frac{\frac{3}{16}\sqrt{\frac{2\pi}{\mu k_b T}}ze}{N_0 K_0}$$

Equation 2 $$Average\ DAR = \frac{[(DAR1*1)+(DAR2*2)+(DAR3*3)\ldots]}{[(DAR0)+(DAR1)+(DAR2)+(DAR3)\ldots]}$$

NISTmAb Charge Variant Analysis

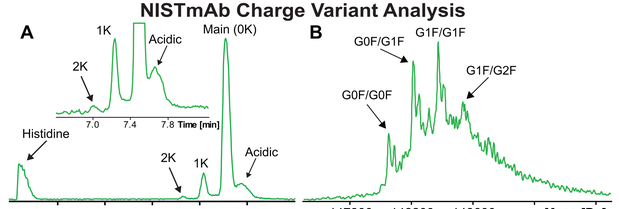

Peak	CCS [Å²]	Mobility 1/K0	CCS Stdv [Å²]	Mobility Resolution 1/K0	Relative Abundance (%)
2K	6021.8	1.15	68.6	29.575	1.4
1K	6233.3	1.197	47.7	17.492	9.6
Main Peak (0K)	6233.7	1.197	16.2	43.916	80.7
Acidic	6190.5	1.189	48.0	17.264	8.3

Figure 1. Native microchip CE-TIMS-MS analysis of NISTmAb in histidine buffer at pH 7. The total ion electropherogram (A) shows separation of NISTmAb products from histidine buffer salt, and four mAb peaks: the double-lysinated NISTmAb (2K), singly lysinated NISTmAb (1K), fully lysine clipped NISTmAb (Main, 0K) and a deamidated acidic charge variant (Acidic). The deconvoluted MS1 spectra of the main peak reveals all four of the expected glycoforms for NISTmAb (B). The exctracted ion mobilograms for each peak (C) shows a shift in the mobility of charge variant peaks which is also reflected in the calculated $^{TIMS}CCS_{N2}$ for each region (D). Interestingly, the 2K peak shows a significantly smaller $^{TIMS}CCS_{N2}$ than the main peak (p=0.009), but neither the 1K or the Acidic peaks are significantly altered when compared to the main peak. Determined CCS for the 1K, main peak, and acidic variant are in good agreement with the global CCS of NISTmAb determined by direct infustion ($^{TIMS}CCS_{N2}$= 6190 Å²) by TIMS[3] and TWIMS[7].

Model Therapeutic mAb

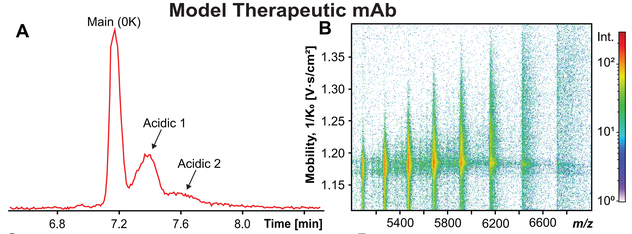

Figure 1. Native microchip CE-TIMS-MS analysis of model therapeutic mAb in histidine buffer at pH 7 with 6% sucrose. The total ion electropherogram (A) shows three mAb peaks: the fully lysine clipped mAb (Main, 0K) and two deamidated acidic charge variants (Acidic 1 and Acidic 2). A heatmap of mobility and *m/z* for the main peak shows limited dependence of mobility on charge state (B). The exctracted ion mobilograms for each peak (C) shows a shift in the mobility of charge variant peaks which is also reflected in the calculated $^{TIMS}CCS_{N2}$ for each region (D), with the Acidic 1 variant showing a significantly larger $^{TIMS}CCS_{N2}$ than the main peak (p=0.002). The results support previous spectroscopic studies of the impact of deamidation on mAb conformation[4,5].

Model Therapeutic Cysteine-Linked ADC

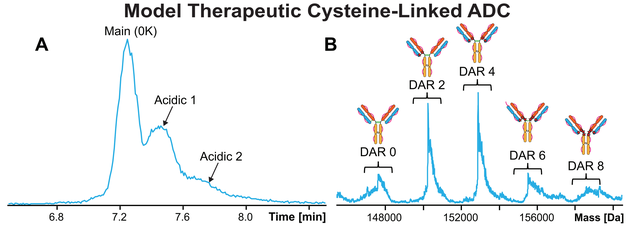

Figure 3. Native microchip CE-TIMS-MS analysis of model therapeutic cysteine-linked ADC in histidine buffer at pH 7. The total ion electropherogram (A) shows three peaks: the fully lysine clipped ADC (Main, 0K) and two deamidated acidic charge variants (Acidic 1 and Acidic 2). Deconvoluted MS1 spectra (B) confirms even drug loading (DAR 0, 2, 4, 6, 8). A heatmap of the ion mobilty and *m/z* shows overlapping species in both the TIMS and MS domains(C). Unlike the mAb, $^{TIMS}CCS_{N2}$ of the first ADC deamidation peak is not significantly different to the main peak. However, the Acidic 2 variant shows $^{TIMS}CCS_{N2}$ values signifcantly larger than either the main peak (p=0.001) or Acidic 1(p=0.004). This indicates that the Acidic 2 variant may destabilize the ADC more than the parent mAb.

Impact of Charge Variants on CCS and DAR

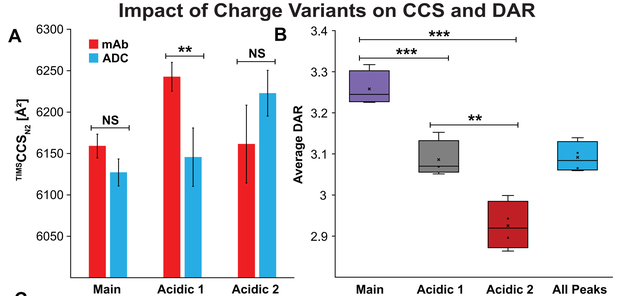

Figure 4. Impacts of charge variant species on measured $^{TIMS}CCS_{N2}$ and average DAR value. Comparison of the measured $^{TIMS}CCS_{N2}$ for the model therapeutic mAb and ADC revealed a significant difference (p=0.009) in the $^{TIMS}CCS_{N2}$ of the first acidic variant (A). The calculated average DAR values for charge variants of the ADC (B) showed significant changes in the average DAR for all comparison points (Main-Acidic 1: p=0.003; Main-Acidic 2: p=0.001; Acidic 1-Acidic 2: p=0.006). The average DAR calculated across all charge variant peaks aligns with previously determined values[3]. Plotting the $^{TIMS}CCS_{N2}$ and average DAR for each charge variant of the model cysteine-linked ADC (C) underscores the opposing trends observed: deamidation variants show an increase in CCS, but decrease in average DAR.

Model Therapeutic Lysine-linked ADC

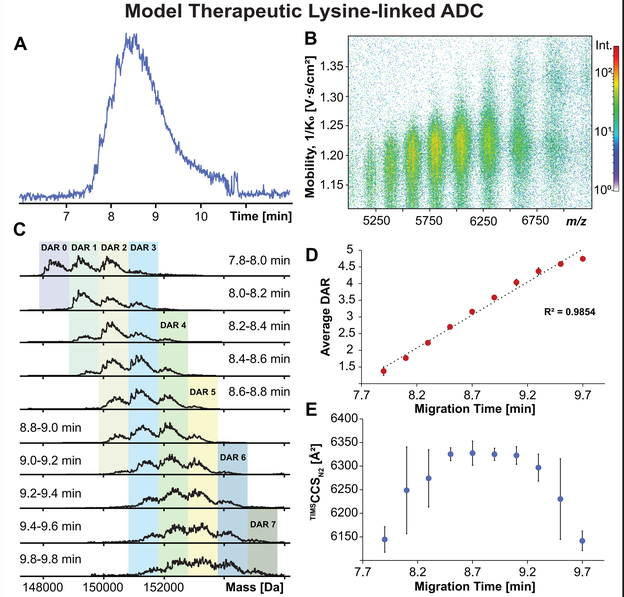

Figure 5. Native microchip CE-TIMS-MS analysis of the lysine-linked ADC, Kadcyla, in histidine buffer at pH 7. The total ion electropherogram (A) shows that charge variants, whether caused by modifications or drug conjugation events, are not fully resolved due to the extreme complexity of the sample. A mobility vs m/z heatmap from 8.6-8.8 minutes migration time (B) show the heterogenity of overlapping charge states and overall low signal for unique DAR species due to drug product heterogenity. The charge deconvoluted MS1 spectra of ten 0.2 minute migration regions (C) demonstrates that as migration time increases, high DAR species (DAR 4-7) are predominantly observed. Considering the average DAR for each migration region reveals a very strong linear correlation between migration time and average DAR indicating partial separation by level of drug conjugation, though DAR species are unresolved (D). The $^{TIMS}CCS_{N2}$ calculated for each migration region exhibits larger standard deviations than those observed for the mAbs and cystine-linked ADC, potentially due to coelution of multiple charge variant species (E).

Conclusion

The combination of microchip capillary electrophoresis and trapped ion mobility enable a rapid, informative method for native monoclonal antibody and antibody-drug conjugate charge variant analysis. Our method allowed detection of significant $^{TIMS}CCS_{N2}$ changes between the unmodifed main peak and deamidated peaks, and can be used to identify charge variants that pose a threat to overall drug stability. Leveraging the powerful combination of a rapid, native liquid-phase separation with TIMS, our approach provides a new tool for pre- and post-clinical quality control which can serve as a foundation to address the ever more complex array of antibody-based therapeutics currently under development.

References

1) Khawli, L. A. *et al. mAbs.* **2010**, 6, 613-624.
2) Wu, Z. and Wang, H. et al. J. Pharm. Biomed. Anal. 2023, 223, 115147
3) Larson, E. J. and Roberts, D. S. et al. Anal. Chem. 2021. 93, 10013-10021.
4) Lu, X. et al. mAbs. 2018. 11, 45-57.
5) Lu, X. et al. Sci. Rep. 2020, 10, 383.
6) Gabelica, V. *et al. Mass Spectrom. Rev.* **2019**, 38, 291-320.
7) Upton, R. *et al. Chem. Sci.* 2019. 10, 2811-2820.

Acknowledgements

The authors acknowledge the support of NIH grants R01HL109810-05A1 R01GM125085, R01HL109810, and R01HL096971.